Accepted Manuscript

Optimization of the nucleation-site density for the electrodeposition of cadmium sulfide on indium-tin-oxide

Sheng Shen, Xiaoyue Zhang, Syed Mubeen, Manuel P. Soriaga, John L. Stickney

PII:	S0013-4686(19)31053-9
DOI:	10.1016/j.electacta.2019.05.120
Reference:	EA 34261
To appear in:	*Electrochimica Acta*
Received Date:	05 April 2019
Accepted Date:	23 May 2019

Please cite this article as: Sheng Shen, Xiaoyue Zhang, Syed Mubeen, Manuel P. Soriaga, John L. Stickney, Optimization of the nucleation-site density for the electrodeposition of cadmium sulfide on indium-tin-oxide, *Electrochimica Acta* (2019), doi: 10.1016/j.electacta.2019.05.120

Electrochimica Acta
Revised Version Submitted May 2019

OPTIMIZATION OF THE NUCLEATION-SITE DENSITY FOR THE ELECTRODEPOSITION OF CADMIUM SULFIDE ON INDIUM-TIN-OXIDE

Sheng Shen[1,2], Xiaoyue Zhang[2], Syed Mubeen[3], Manuel P. Soriaga[4] and John L. Stickney[2,*]

[1]College of Chemistry and Chemical Engineering
Hunan University
Changsha, Hunan, 410082 People's Republic of China

[2]Department of Chemistry
University of Georgia
Athens, GA 30602 USA

[3]College of Engineering
University of Iowa
Iowa City, IA 52242 USA

[4]Joint Center of Artificial Photosynthesis
California Institute of Technology
Pasadena, CA 91106 USA

* To whom correspondence should be addressed. Email address: stickney@uga.edu,

ABSTRACT

Cadmium sulfide (CdS) is a preferred heterojunction partner for a number of chalcogenide-based solar cells. In view of this, interest has grown in the use of solution-based deposition techniques as an alternative route for the preparation of uniform ultrathin films of CdS. However, the quality of the electrodeposited CdS films on indium-tin oxide (ITO) remains far from optimal. This is because the ITO surface is electrochemically heterogeneous due to the presence of indium oxide; nucleation and further electrodeposition of CdS does not transpire on the oxided sites. Hence, only coarse-grained coatings, instead of homogeneous ultrathin films, are generated at un-pretreated ITO surfaces. In the present study, a mitigation of the amount of interfacial In oxide was attempted in order to increase the nucleation-site (indium-metal site) density. The procedure consisted of two steps: (i) Mild electrochemical reduction of the ITO to convert surface In(III) to In(0), followed by (ii) surface-limited redox replacement (SLRR) of In(0) by Cu via an aqueous solution of Cu^{2+}. This procedure resulted in the formation of a high density of oxide-free Cu on which CdS nuclei would form; the thickness was such that optical transparency was largely undiminished. A ten-fold increase in CdS site density was observed, and that permitted the epitaxial growth of a second semiconductor, CdTe, atop the CdS film. The influences of applied potential and deposition time on nucleation-site sizes and densities were also studied.

Keywords: Indium-tin-oxide

Nucleation and Growth

E-ALD

Cadmium Sulfide

Semiconductor Thin Films

INTRODUCTION

Electrodeposition has been successfully implemented in the syntheses of photovoltaic materials since the 1970s[1]. The unique benefits offered by electrodeposition include: operation under ambient conditions; low-physical footprint; maximization of raw-material utilization; and reasonable control over the quality of the deposit simply by tuning deposition parameters and electrolyte chemistries. Since deposition techniques are applied at ordinary temperatures, they avoid the interdiffusion of material, typical in high-temperature processes, to yield sharper junctions[2]. In a typical superstrate thin-film solar cell configuration, the n-type semiconductor (e.g., CdS) lies above a transparent conducting oxide (TCO), with a p-type absorber layer on top. Over the years, numerous p-type semiconductor materials, such as CdTe[3-5], Cu(In,Ga)Se (CIGS)[6-9], and Cu_2ZnSnS_4 (CZTS)[10-13], have been prepared by electrodeposition. Impressive developments have been made in the electrodeposition of high-quality p-type semiconductors, but improvements in the electrodeposition of the n-type buffer layer on a TCO have not been as dramatic. A major factor is that the TCOs are non-metallic whose surfaces are predominantly oxygen-terminated. This characteristic is rather consequential because electrodeposition occurs only on surface atoms that are metallically (electrically) conductive for electron transfer, and are able to engage in stable substrate-deposit chemical bonds. Such surface atoms are thus the nucleation sites on the polycrystalline TCO surface. Presently, ITO and fluorine-doped tin oxide (FTO) are the most widely used TCO substrates for solar cells, with ITO as the preference due to its advantages in electrical conductivity and optical transmittance. As an n-type semiconductor with a bandgap between 3.5 - 4.3 eV, ITO nominally consists of In_2O_3 with 10% by weight of SnO_2[14]. There may be up to 4 different forms of surface oxygens in ITO, as well as at least two forms of In and Sn[15]. The nature of the oxide in ITO, the extent of hydrolysis of the lattice, and the density and orientation of the oxide grains, can all lead to a fairly high degree of surface heterogeneity. The high concentration of carriers in ITO arises from the various defect sites that include oxygen vacancies, interstitial indium, and substitutional Sn^{4+} at In^{3+} sites[16]. Chemical reactions are to be expected to take place preferentially at the chemically active defect sites. As a result, electrodeposition of CdS on ITO proceeds through a nucleation-and-growth mechanism. The formation of a non-fragmented

coating is dependent upon the density of the nucleation sites, as well as the thickness of the deposit. The higher the nucleation density, the thinner the film can be. Although thin CdS layers lead to a higher J_{sc} due to enhanced shorter-wavelength transmittance, there is a functional limitation to film thinness because unduly thin CdS films are quite susceptible to pinholes that serve to reduce V_{oc} and FF[17]. In actuality, it is the nucleation density that ultimately controls the generation of optimally thin CdS layers, and, by extension, helps to dictate the overall performance of the solar cell.

The Stickney group has been working on the electrodeposition of semiconductors for the better of two decades, and has led the development of electrochemical of atomic layer deposition (E-ALD)[18-25]. Analogous to gas-phase ALD, E-ALD takes advantage of a surface-limited reaction to deposit one atomic layer at a time. The surface-limited reaction in E-ALD is simply underpotential deposition (UPD), in which one element deposits on a second element before it deposits onto itself; the reaction is driven by the decrease in free energy associated with the surface-compound formation[26-27]. UPD is observed with Cd and S on metals such as Au[28-29], Ag[30-32], and Cu[33-34]. These metal surfaces are characterized by a homogeneous reservoir of electrons that enable rapid electron exchanges at any point on the surface. However, as previously mentioned, species such as Cd or S have little chemical affinity towards oxygen atoms or hydroxyl species at the surface of ITO. Hence, electrodeposition on ITO takes place only at sites devoid of oxygenous groups; i.e, the nucleation sites.

SILAR, or successive ionic layer adsorption and reaction, a process similar to E-ALD, has also been attempted by the Stickney group to prepare CdS on ITO. In SILAR, the substrate goes through alternate immersions of the precursor (e.g., Cd^{2+} and S^{2-}) solutions, where each immersion results in the precipitation or deposition of less than one monolayer of material. However, when CdTe was deposited[1] by E-ALD onto a SILAR-fabricated CdS/ITO, delamination of CdS/CdTe from the ITO substrate was invariably observed. Figure 1 shows the scanning electron microscopy (SEM) image that illustrates the delamination of the CdS/CdTe layer. A possible explanation is that SILAR creates deposits via

[1] Deposition of CdTe is discussed in a separate paper [J. Electrochem. Soc. 166 (2019) H3249-H3256].

precipitation of the precursor ions ($Cd^{2+} + S^{2-} \rightarrow CdS$) but there is no real chemical interaction between the film and the substrate. Evidently, the weak adhesion between the SILAR-fabricated CdS and the ITO substrate is not enough to overcome the stress exerted by the CdTe overlayer; consequently, the film buckles. In order to synthesize a CdTe/CdS photovoltaic assembly, other approaches to form CdS/ITO have to be explored.

After the seminal paper[35] that demonstrated the influence of applied potential on the composition of indium oxide was published, the electrochemical reduction of ITO has been studied with different electrolytes at different pHs[16, 36-45]; most of the studies focused on the electrochemical stability of ITO, rather than the influence of surface modifications. In 2014, Switzer et al., successfully deposited Ge wires by first reducing ITO to form In metal that acted as reduction sites for Ge (IV)[46]. This work pointed to the direction that, if a pre-reduction is performed to the surface of ITO, the resulting In metal can be used as nucleation sites for CdS electrodeposition. The degree of reduction dictates the number of surface elemental In, but an excess of reduction can lead to the loss of transparency and conductivity of ITO. By careful control of the reduction time and potential, the nucleation site density can be maximized without alteration of the nature of bulk ITO. The In sites provide a metallic surface for CdS spherical layer-by-layer growth. As the coverage grows, the film coalesces and eventually covers the entire surface. The In atoms can also serve as anchor points and promote better adhesion between CdS and ITO. The denser the nucleation sites are, the better the film adhesion ought to be.

It must be pointed out that the Pourbaix diagrams of Cd and In indicate that, at potentials where Cd undergoes electrodeposition, metallic In is on the verge of being oxidized. This is confirmed by the cyclic voltammetric (CV) and SEM data described in later sections. A more stable metal should thus be used to in lieu of In as the nucleation site. The plan proposed in this study is to employ Cu as a replacement for In; the substitution procedure is straightforward via a redox displacement reaction between Cu^{2+} and In: $3\ Cu^{2+} + 2\ In \rightarrow 3\ Cu + 2\ In^{3+}$ at open circuit. The effects of trace amounts of Cu on the CdS/ITO interface is not completely understood at this time, but CdS thin films doped with metals

such as Sn[47-48], Ga[49], Ag[50-51], Cu have been investigated. It has been reported that the use of Cu as a dopant of CdS allows for a decrease in the thickness of CdS from 70 nm to 30 nm, with the same high-efficiency[52]; an increase in transmittance with Cu-doped CdS was also reported[53]. Thus Cu was chosen as the metal to replace indium.

EXPERIMENTAL

All potentials are reported against a Ag/AgCl (3 M KCl) reference electrode (Bioanalytical Systems, Inc., West Lafayette, IN). The ITO substrates (Delta Technologies, Ltd., Loveland, CO) with sheet resistance, R_s, of 70-100 Ω/sq, were cleaned prior to use by three 15-min sonication treatments in fresh aliquots of acetone and then in three aliquots of Milli-Q® Advantage A10 water (MilliporeSigma, Burlington, MA). The Cd^{2+} solution of pH 3, and contained 0.5 mM $CdSO_4$ (Sigma-Aldrich Corp., St. Louis, MO) in 0.5 M $NaClO_4$. The sulfide solution was at pH 10.5, with 0.5 mM Na_2S (J. T.Baker, VWR International, Visalia, CA) in 0.5 M $NaClO_4$. The Cu^{2+} solution, set at pH 3, had 0.5 mM $CuSO_4$ (J. T.Baker) in 0.5 M $NaClO_4$. The electrolyte-only wash solutions consisted of 0.5 M $NaClO_4$ at pH 3 and pH 10.5 respectively, for the acid and base rinses. All solutions were made using 18 MΩ Milli-Q® water.

All electrochemical experiments were carried out in a flow-cell system (Electrochemical ALD, L.C., Athens, GA) that consisted of a distribution valve, a flow cell, a pump, and a three-electrode potentiostat. The system was automated by an in-house LabVIEW-based program named Sequencer. The auxiliary electrode was a Au wire embedded in the cell wall that faced the ITO working electrode. The exposed electrode area was 2.1 cm^2. The flow rate for the ITO pre-treatments, and for all CV runs, was kept 2 mL/min. The flow rate for the deposition of CdS deposition was maintained at 11 mL/min for the entire process. CVs were performed at a scan rate of 10 mV/s. All solutions were purged with N_2 prior to and during the experiment.

Transmittance spectra were obtained with a Thermo Fisher Evolution 260 Bio UV-Visible spectrophotometer (Thermo Fisher, Waltham, MA), with an integration time of 0.05 s, and a scan speed

of 1200 nm/min. Scanning electron microscopy and energy dispersive X-ray spectroscopy (SEM-EDX) were performed on an FEI Teneo SEM (FEI, Hillsboro, OR) with an acceleration voltage of 10 keV.

RESULTS AND DISCUSSION

1) ITO reduction by cathodic treatment

Figure 2 displays the current-vs-potential curves for ITO in 0.5 M $NaClO_4$ solution at pH 3, scanned initially in the negative direction from the open-circuit potential, 0.60 V. No sign of reduction was observed in the first (blue) scan, down to the reversal potential at -0.800 V. When the scan was extended to -0.900 V (purple scan and in the inset of Figure 2), a small oxidation peak was observed positive to -600 mV that corresponds to re-oxidation of the reduced In to its oxide state. Unfortunately, because of the competition by the hydrogen evolution reaction (HER), the total current remained in the cathodic regime. As the negative limit was pushed to -1000 mV (red scan), The oxidation peak positive of -650 mV, for In oxidation, grew dramatically. No reduction and re-oxidation peak of Sn was observed, consistent with the literature[38]. To minimize changes in the ITO, a reduction potential of -900 mV was chosen so as to result in only surface modification.

Figure 3 shows anodic scans for ITO after reduction at -900 mV for 10 s, 30 s and 90 s. The anodic peak positive to -600 mV, corresponds to the In(0) to In(III) reaction. Integration of the peak provided the oxidation charge which enabled the quantification of the metallic indium; that charge increased linearly with reduction time (Figure 3, inset). Integration of the In in the black scan suggested the equivalent of 4 ML of In (1 ML In is roughly 1386 μC for a 2.1 cm^2 electrode), based on the three-electron In(III)-to-In(0) process. The SEM image in Figure 4(c) indicated a non-uniform distribution.

To determine the effect of the In(III) reduction on the morphology of the CdS-ITO surface, SEM images were taken as a function of the ITO-reduction time; the results are shown in Figure 4 for three samples reduced at -900 mV for 60 s, 90 s, and 180 s, along with that for an untreated ITO as reference. The reduction led to the formation of surface pits and clusters, the number of which increased with the length of the reduction time. The clusters were identified by EDX and found to be considerably higher in the quantity of In relative to that in the background (Figure 5). But the post-reduction sizes of the

nucleation sites were smaller, which is a desired result. Prolonged reduction (180 s) was deemed excessive because the ITO became visibly gray and opaque; the loss of transparency, of course, leads to inferior photovoltaic performance. Hence, 90 s was chosen as the most appropriate reduction time. The sizes of the bright spots in a 1μm^2 area [Figure 4(b)] were assumed to be hemispherical; this allowed the number of In atoms to be calculated from the total volume based on the density of In. Such approximation suggested about 3 ML of In; in comparison, 4 ML was indicated by coulometry. The difference is likely because not all the nucleation sites are viewable in the SEM images; the heterogeneity in the distribution across the deposit surface should also be a contributor to the discrepancy.

Figure 6(a) is a zoomed-in SEM of ITO reduced at -900 mV for 90 s but emersed as soon as the reduction time was reached. As evident in the image, the In clusters appeared to form immediately adjacent to the pits. A possible explanation is that reduction was initiated at the grain boundaries[37, 44, 54], where the In oxide was slowly reduced to metal that led to pit formation; the In metal then aggregated in clusters next to the pits. The In clusters were found to be unstable, and eventually dissolved away when left in the blank. Proof can be seen in Figure 6(b), an SEM imaged of ITO reduced at -900 mV for 90 s and consigned to a blank solution at open circuit for 5 min; the In clusters have dissolved, leaving only pits on the surface.

2) Deposition of copper nuclei by redox displacement

To overcome the poor stability of the In nucleation sites, a fraction of the In was substituted by Cu, a less reactive metal, via a redox displacement reaction with aqueous Cu^{2+} solution: $3Cu^{2+}_{(aq)} + 2In_{(s)} \rightarrow 3Cu_{(s)} + 2In^{3+}_{(aq)}$. To confirm the co-existence of Cu metal in the tin oxide, cathodic-stripping voltammetry for Cu was performed (Figure 7) starting at the OCP (0.10 V); Cu dissolution occurred at 100 mV. The black curve was obtained after 5 min of redox replacement in Cu^{2+} solution at open circuit. Positive of the bulk stripping peak, the current did not drop to zero, but was maintained at about 50 µA; no such current plateau was observed for the Cu^{2+}-free control solution (red curve). This clearly indicated that that the vestigial current at E > 0.10 V was due to the presence of Cu probably stabilized by bonds to to the substrate but not to other (bulk) Cu atoms. It appears that most of the Cu replacements can be

stripped at 200 mV, with a fraction of the Cu atoms remaining bonded to the nucleation sites on the modified ITO surface.

SEM was performed on the ITO substrates at different stages of the above treatment. Figure 8(a) displays ITO after 90 s of reduction, while 8(b) displays ITO after 90 s of reduction plus 5 min of $CuSO_4$ exchange at open circuit; under the conditions of Figure 8(b), no obvious changes in the density or distribution of the clusters were observed. In Figure 8(c), however, the clusters were no longer visible; clearly, the the majority of the exchanged Cu had been stripped at 200 mV; only the Cu that was still bonded to the ITO substrates remained .

To investigate how pre-treatment of the ITO substrate affected the nucleation density, bulk Cd was deposited at -900 mV for 90 s on both untreated ITO and the Cu-treated ITO; the results are shown in Figure 9. The SEM image in Figure 9(a) is for an untreated ITO image after Cd deposition; only a small number of appreciably large Cd clusters appeared. On the Cu-treated substrate, Figure 9(b), the Cd clusters were smaller but of a much higher density. Figures 9(c) and 9(d) are histograms[55] that indicate the size distributions of the particles in Figures 9(a) and 9(b), respectively. A tally of the clusters over an area of 9 μm^2 revealed that there the population of clusters (424) for the treated ITO is ten-fold more than that (33) for the unreated substrate); it can thus be concluded that the Cu-for-In exchange treatment significantly increases the nucleation density in ITO.

Transmittance spectra were acquired to ascertain if the Cu-In-exchange treatment had any effect on the transparency of the ITO. Figure 10 shows a plot of the % transmittance as a function of wavelength for untreated ITO (black) and Cu-exchanged ITO (red) between 200 to 1100 nm. The post-Cu-treatment plot was slightly but noticeably lower by 4% in transmittance that for the unsubstituted ITO.

3) CdS deposition by E-ALD cycles

It may seem paradoxical but the ITO pretreatment described above, *viz*., 90 s of ITO reduction at -900 mV, followed by a 5 min open-circuit exposure to $CuSO_4$, and concluded with an anodic scan in $CuSO_4$ to 200 mV, resulted in a substrate surface with a minimum coverage of Cu coverage, yet the

population of semiconductor-deposition nucleation sites, which had been the In sites substituted with Cu atoms, has been substantially increased. Subsequent E-ALD of a CdS thin film was then carried out on the chemically modified ITO surface, as detailed elsewhere[56]. In a single E-ALD cycle, Cd and S precursor ions were introduced in separately with each deposited at its own UPD potential, such that the deposits were formed with self-terminating reactions on the nucleation sites. That is, each cycle resulted in the deposition of less than one atomic layer, on only nucleation sites, per cycle, that served to eliminate coarse-grain formation; one adsorbate atom per substrate surface atom was used to define a monolayer. The precursor solutions were rinsed away with pure supporting electrolyte between each deposition step. As the number of cycles repeats, the deposited monolayers grow and coalesce into a continuous film. The deposition potentials and times have been systematically studied and optimized previously[56]. Figure 11 is an illustration of one complete E-ALD cycle. The black and red traces show the programmed potential on the left axis, and the resulting current on the right axis, respectively. The solutions in the cell for each step are marked in green. Potentials were altered 2 seconds after initiation of the solution change, enough time for exchange in the cell.

Figure 12 displays SEM images of ITO reduced at -900 mV for 90 s after (a) 50 cycles of CdS deposition on a Cu-treated substrate, and (b) 50 cycles of CdS deposition on untreated ITO. Most of the surface Cu atoms in the deposit in (a) were covered by the CdS, whereas the surface in (b) showed a much lower number of clusters of Cu-free ITO. In Figure 12(a), the areas external to the nucleation sites appear to have a coarse texture, distinctly different from that of the uncoated surface, seen to be smooth in Figure 12(b). The uneven appearance suggests the formation of secondary nucleation sites upon coalescence of the larger primary CdS particles.

The creation of secondary nucleation sites raises a few questions with regard to the CdS nanofilms. (a) If the ITO is not completely covered, is the quality of the junction between CdS and the second deposit, CdTe, degraded? (b) If parts of the ITO remain oxygen-terminated, is deposition at those spots inhibited, or would the absorber layer still deposit there; if so, how would the p-n junction be affected? (c) If the absorber layer spreads only across the CdS sites, would it be possible for electron

transfer to occur from CdS into ITO, via the junctions at the original nucleation sites? (d) Given sufficient density of CdS/ITO sites, would the junctions be accessible for facile electron transfer, while the ITO areas devoid CdS sites would be bypassed? These are issues that will need to be explored in future work.

A sequence of CdS deposits formed from different numbers of E-ALD cycles on the Cu-treated ITO are also displayed in Figure 12: (c) 5 cycles, (d) 15 cycles and (e) 25 cycles. The CdS growth in (c) appears to be initiated adjacent to pits, created during the initial ITO reduction step, suggesting deposits originated at sites where metallic In was formed but subsequently exchanged with Cu. As the deposit expanded, nucleation sites at the smooth areas emerged, suggesting that smaller nucleation sites, not observable initially due to their puny sizes, were also generated on those smoother areas. In the absence of Cu exchange, the smaller nucleation sites were much less numerous, Figure 12(b). In Figure 12(e), it can be seen that the deposit formed not only on the nucleation sites next to the pits but also on the smooth planar areas. The layer-by-layer growth of roughly hemispherical CdS particles eventually coalesced, producing a continuous film. The Cd/S atomic ratio of 0.8 from EDX indicated a S-deficient, n-type, CdS.

Investigations into the stability of the CdS/ITO interface as a function of the pretreatment were carried out by electrodeposition of CdTe on the CdS films. Figure 13 shows SEM images of 50 cycles of CdS on a Cu-treated ITO substrate, before and after 90 cycles of pulse-plated atomic layer deposition (PP-ALD)[57] of CdTe. The CdTe/CdS/Cu-ITO structure displayed larger size grains and did not peel off, in contrast to that without the Cu-exchange treatment. Increasing number of cycles to 360 for the CdTe deposition also resulted in a stable structure, with no evidence of delamination.

CONCLUSION

Reduction of an appreciable amount of In(III) to metallic In(0) in ITO, followed by its exchange with Cu via surface-limited redox replacement in Cu^{2+} solution, resulted in a ten-fold increase in the number of semiconductor-deposition nucleation sites on the ITO surface. Studies of the deposition of CdS and CdS-on-CdTe nanofilms on the reduced ITO surface by E-ALD were then pursued. Previous work had shown a lack of adhesion between the CdTe-on-CdS deposit and the ITO substrate, and the absence of adhesion led to prompt delamination of the deposit. When Cu-exchange was undertaken, no delamination was observed. Evidently, the increase in nucleation density led to the formation of homogeneous CdS sites which, in turn, facilitated the deposition of a nanofilm of adherent CdTe.

AUTHOR INFORMATION

Corresponding Author

*stickney@uga.edu *

Author Contributions

The manuscript was written through contributions of all authors. All authors have given approval to the final version of the manuscript.

Funding Sources

DMR 1410109

ACKNOWLEDGMENT

Support from the National Science Foundation, DMR 1410109, is gratefully acknowledged. Thanks are extended to the Georgia Electron Microscopy for use of their SEM and Dr. Ryan Hilli's group for their spectrophotometer. The Joint Center for Artificial Photosynthesis at the California Institute of Technology, a DOE Energy Innovation Hub, supported through the Office of Science of the U.S. Department of Energy (DE-SC0004993), provided assistance for Professor M. P. Soriaga. We thank Dr. Andrea Resta, Synchrotron Soleil, L'Orme des Merisiers, Gif-sur-Yvette, France for his contributions to this work.

REFERENCES

1. Kröger, F. A., Cathodic Deposition and Characterization of Metallic or Semiconducting Binary Alloys or Compounds. *J. Electrochem. Soc.* **1978,** *125* (12), 2028-2034.

2. Lokhande, C.; Pawar, S., Electrodeposition of thin film semiconductors. *physica status solidi (a)* **1989,** *111* (1), 17-40.

3. Sella, C.; Boncorps, P.; Vedel, J., The electrodeposition mechanism of CdTe from acidic aqueous solutions. *J. Electrochem. Soc.* **1986,** *133* (10), 2043-2047.

4. Barker, J.; Binns, S.; Johnson, D.; Marshall, R.; Oktik, S.; Özsan, M.; Patterson, M.; Ransome, S.; Roberts, S.; Sadeghi, M., Electrodeposited CdTe for thin film solar cells. *International journal of solar energy* **1992,** *12* (1-4), 79-94.

5. Diso, D.; Fauzi, F.; Echendu, O.; Olusola, O.; Dharmadasa, I., Optimisation of CdTe electrodeposition voltage for development of CdS/CdTe solar cells. *Journal of Materials Science: Materials in Electronics* **2016,** *27* (12), 12464-12472.

6. Saji, V. S.; Choi, I.-H.; Lee, C.-W., Progress in electrodeposited absorber layer for CuIn (1− x) GaxSe 2 (CIGS) solar cells. *Sol. Energy* **2011,** *85* (11), 2666-2678.

7. Calixto, M.; Sebastian, P.; Bhattacharya, R.; Noufi, R., Compositional and optoelectronic properties of CIS and CIGS thin films formed by electrodeposition. *Sol. Energy Mater. Sol. Cells* **1999,** *59* (1), 75-84.

8. Bhattacharya, R. N.; Oh, M.-K.; Kim, Y., CIGS-based solar cells prepared from electrodeposited precursor films. *Sol. Energy Mater. Sol. Cells* **2012,** *98*, 198-202.

9. Lincot, D.; Guillemoles, J.-F.; Taunier, S.; Guimard, D.; Sicx-Kurdi, J.; Chaumont, A.; Roussel, O.; Ramdani, O.; Hubert, C.; Fauvarque, J., Chalcopyrite thin film solar cells by electrodeposition. *Sol. Energy* **2004,** *77* (6), 725-737.

10. Pawar, S.; Pawar, B.; Moholkar, A.; Choi, D.; Yun, J.; Moon, J.; Kolekar, S.; Kim, J., Single step electrosynthesis of Cu 2 ZnSnS 4 (CZTS) thin films for solar cell application. *Electrochim. Acta* **2010,** *55* (12), 4057-4061.

11. Ahmed, S.; Reuter, K. B.; Gunawan, O.; Guo, L.; Romankiw, L. T.; Deligianni, H., A high efficiency electrodeposited Cu2ZnSnS4 solar cell. *Advanced Energy Materials* **2012,** *2* (2), 253-259.

12. Scragg, J. J.; Dale, P.; Peter, L. M., Synthesis and characterization of Cu 2 ZnSnS 4 absorber layers by an electrodeposition-annealing route. *Thin Solid Films* **2009,** *517* (7), 2481-2484.

13. Gurav, K.; Yun, J.; Pawar, S.; Shin, S.; Suryawanshi, M.; Kim, Y.; Agawane, G.; Patil, P.; Kim, J., Pulsed electrodeposited CZTS thin films: Effect of duty cycle. *Materials Letters* **2013,** *108*, 316-319.

14. Kim, H.; Gilmore, C.; Pique, A.; Horwitz, J.; Mattoussi, H.; Murata, H.; Kafafi, Z.; Chrisey, D., Electrical, optical, and structural properties of indium–tin–oxide thin films for organic light-emitting devices. *J. Appl. Phys.* **1999,** *86* (11), 6451-6461.

15. Donley, C.; Dunphy, D.; Paine, D.; Carter, C.; Nebesny, K.; Lee, P.; Alloway, D.; Armstrong, N. R., Characterization of Indium−Tin Oxide Interfaces Using X-ray Photoelectron Spectroscopy and Redox Processes of a Chemisorbed Probe Molecule: Effect of Surface Pretreatment Conditions. *Langmuir* **2002,** *18* (2), 450-457.

16. Bejitual, T. S.; Ramji, K.; Kessman, A. J.; Sierros, K. A.; Cairns, D. R., Corrosion of an amorphous indium tin oxide film on polyethylene terephthalate at low concentrations of acrylic acid. *Materials Chemistry and Physics* **2012,** *132* (2–3), 395-401.

17. Nakamura, K.; Gotoh, M.; Fujihara, T.; Toyama, T.; Okamoto, H., Influence of CdS window layer on 2- μ m thick CdS/CdTe thin film solar cells. *Sol. Energy Mater. Sol. Cells* **2003,** *75* (1), 185-192.

18. Gregory, B. W.; Stickney, J. L., Electrochemical atomic layer epitaxy (ECALE). *Journal of electroanalytical chemistry and interfacial electrochemistry* **1991,** *300* (1-2), 543-561.

19. Tsang, C. F.; Ledina, M. A.; Stickney, J. L., Molybdenum diselenide formation using electrochemical atomic layer deposition (E-ALD). *J Electroanal Chem* **2017**.

20. Perdue, B.; Czerniawski, J.; Anthony, J.; Stickney, J., Optimization of Te Solution Chemistry in the Electrochemical Atomic Layer Deposition Growth of CdTe. *J. Electrochem. Soc.* **2014,** *161* (7), D3087-D3092.

21. Banga, D.; Perdue, B.; Stickney, J., Formation of CuIn(1-x)GaxSe2 (CIGS) by Electrochemical Atomic Layer Deposition (ALD). *J. Electrochem. Soc.* **2014,** *161* (4), D141-D146.

22. Thambidurai, C.; Kim, Y. G.; Jayaraju, N.; Venkatasamy, V.; Stickney, J. L., Copper Nanofilm Formation by Electrochemical ALD. *J. Electrochem. Soc.* **2009,** *156* (8), D261-D268.

23. Venkatasamy, V.; Stickney, J. L., Formation of HgCdTe by Electrochemical Atomic Layer Epitaxy (EC-ALE). *ECS Transactions* **2006,** *3* (accepted).

24. Venkatasamy, V.; Jayaraju, N.; Thambidurai, C.; Cox, C.; Happek, U.; Stickney, J. L., Optimization studies of CdTe nanofilm formation by electrochemical atomic layer epitaxy (EC-ALE). *J. Appl. Electrochem.* **2006,** *36*, 1223.

25. Mathe, M. K.; Cox, S. M.; Flowers, B. H.; Vaidyanathan, R.; Pham, L.; Srisook, N.; Happek, U.; Stickney, J. L., Deposition of CdSe by EC-ALE. *Journal of Crystal Growth* **2004,** *271* (1-2), 55-64.

26. Gregory, B. W.; Norton, M. L.; Stickney, J. L., Thin-layer electrochemical studies of the underpotential deposition of cadmium and tellurium on polycrystalline Au, Pt and Cu electrodes. *J Electroanal Chem* **1990,** *293* (1-2), 85-101.

27. Gregory, B. W.; Stickney, J. L., Electrochemical atomic layer epitaxy (ECALE). *J Electroanal Chem* **1991,** *300* (1-2), 543-561.

28. Colletti, L. P.; Flowers, B. H.; Stickney, J. L., Formation of thin films of CdTe, CdSe, and CdS by electrochemical atomic layer epitaxy. *J. Electrochem. Soc.* **1998,** *145* (5), 1442-1449.

29. Lay, M. D.; Varazo, K.; Stickney, J. L., Formation of Sulfur Atomic Layers on Gold from Aqueous Solutions of Sulfide and Thiosulfate: Studies Using EC-STM, UHV-EC, and TLEC. *Langmuir* **2003,** *19* (20), 8416-8427.

30. Foresti, M. L.; Milani, S.; Loglio, F.; Innocenti, M.; Pezzatini, G.; Cattarin, S., Ternary CdSxSe1-x deposited on Ag(111) by ECALE. Synthesis and characterization. *Langmuir* **2005,** *21* (15), 6900-6907.

31. Foresti, M. L.; Pezzatini, G.; Cavallini, M.; Aloisi, G.; Innocenti, M.; Guidelli, R., Electrochemical atomic layer epitaxy deposition of CdS on Ag (111): An electrochemical and STM investigation. *J. Phys. Chem. B* **1998,** *102* (38), 7413-7420.

32. Forni, F.; Innocenti, M.; Pezzatini, G.; Foresti, M. L., Electrochemical aspects of CdTe growth on the face of (111) of silver by EC-ALE. *Electrochemica Acta* **2000,** *45* (20), 3225-3231.

33. Stuhlmann, C.; Park, Z.; Bach, C.; Wandelt, K., An ex-situ study of Cd underpotential deposition on Cu(111). *Electrochim. Acta* **1998,** *44* (6), 993-998.

34. Hümann, S.; Hommrich, J.; Wandelt, K., Underpotential deposition of cadmium on Cu(111) and Cu(100). *Thin Solid Films* **2003,** *428* (1), 76-82.

35. Armstrong, N. R.; Lin, A. W.; Fujihira, M.; Kuwana, T., Electrochemical and surface characteristics of tin oxide and indium oxide electrodes. *Analytical Chemistry* **1976,** *48* (4), 741-750.

36. Senthilkumar, M.; Mathiyarasu, J.; Joseph, J.; Phani, K. L. N.; Yegnaraman, V., Electrochemical instability of indium tin oxide (ITO) glass in acidic pH range during cathodic polarization. *Materials Chemistry and Physics* **2008,** *108* (2–3), 403-407.

37. Gao, W.; Cao, S.; Yang, Y.; Wang, H.; Li, J.; Jiang, Y., Electrochemical impedance spectroscopy investigation on indium tin oxide films under cathodic polarization in NaOH solution. *Thin Solid Films* **2012,** *520* (23), 6916-6921.

38. Liu, L.; Yellinek, S.; Valdinger, I.; Donval, A.; Mandler, D., Important implications of the electrochemical reduction of ITO. *Electrochimica Acta* **2015,** *176*, 1374-1381.

39. Spada, E. R.; de Paula, F. R.; Plá Cid, C. C.; Candiotto, G.; Faria, R. M.; Sartorelli, M. L., Role of acidic and basic electrolytes on the structure and morphology of cathodically reduced indium tin oxide (ITO) substrates. *Electrochim. Acta* **2013,** *108*, 520-524.

40. Bouden, S.; Dahi, A.; Hauquier, F.; Randriamahazaka, H.; Ghilane, J., Multifunctional Indium Tin Oxide Electrode Generated by Unusual Surface Modification. *Scientific Reports* **2016,** *6*.

41. Matveeva, E., Electrochemistry of the Indium-Tin Oxide Electrode in 1 M NaOH Electrolyte. *J. Electrochem. Soc.* **2005,** *152* (9), H138-H145.

42. Huang, C. A.; Li, K. C.; Tu, G. C.; Wang, W. S., The electrochemical behavior of tin-doped indium oxide during reduction in 0.3 M hydrochloric acid. *Electrochim. Acta* **2003,** *48* (24), 3599-3605.

43. van den Meerakker, J. E. A. M.; Baarslag, P. C.; Scholten, M., On the Mechanism of ITO Etching in Halogen Acids: The Influence of Oxidizing Agents. *J. Electrochem. Soc.* **1995,** *142* (7), 2321-2325.

44. Huang, C.; Li, K.; Tu, G.; Wang, W., The electrochemical behavior of tin-doped indium oxide during reduction in 0.3 M hydrochloric acid. *Electrochim. Acta* **2003,** *48* (24), 3599-3605.

45. WANG, H.; ZHONG, C.; JIANG, C.-J.; GU, X.; LI, J.; JIANG, Y.-M., Electrochemical Behavior of ITO Films during Anodic and Cathodic Polarization in Sodium Hydroxide Solutions. *Acta Phys.-Chim. Sin.* **2009,** *25* (5), 835-839.

46. Mahenderkar, N. K.; Liu, Y.-C.; Koza, J. A.; Switzer, J. A., Electrodeposited Germanium Nanowires. *ACS Nano* **2014,** *8* (9), 9524-9530.

47. Roy, P.; Srivastava, S. K., In situ deposition of Sn-doped CdS thin films by chemical bath deposition and their characterization. *Journal of Physics D: Applied Physics* **2006,** *39* (22), 4771.

48. Jafari, A.; Zakaria, A.; Rizwan, Z.; Ghazali, M. S. M., Effect of low concentration Sn doping on optical properties of CdS films grown by CBD technique. *International journal of molecular sciences* **2011,** *12* (9), 6320-6328.

49. Khallaf, H.; Chai, G.; Lupan, O.; Chow, L.; Park, S.; Schulte, A., Characterization of gallium-doped CdS thin films grown by chemical bath deposition. *Applied surface science* **2009,** *255* (7), 4129-4134.

50. Shah, N.; Nazir, A.; Mahmood, W.; Syed, W.; Butt, S.; Ali, Z.; Maqsood, A., Physical properties and characterization of Ag doped CdS thin films. *Journal of Alloys and Compounds* **2012,** *512* (1), 27-32.

51. Ristova, M.; Ristov, M., Silver-doped CdS films for PV application. *Sol. Energy Mater. Sol. Cells* **1998,** *53* (1), 95-102.

52. Sánchez, Y.; Espíndola-Rodríguez, M.; Xie, H.; López-Marino, S.; Neuschitzer, M.; Giraldo, S.; Dimitrievska, M.; Placidi, M.; Izquierdo-Roca, V.; Pulgarín-Agudelo, F. A.; Vigil-Galán, O.; Saucedo,

E., Ultra-thin CdS for highly performing chalcogenides thin film based solar cells. *Sol. Energy Mater. Sol. Cells* **2016,** *158*, 138-146.

53. Shah, N. A.; Sagar, R. R.; Mahmood, W.; Syed, W. A. A., Cu-doping effects on the physical properties of cadmium sulfide thin films. *Journal of Alloys and Compounds* **2012,** *512* (1), 185-189.

54. Choi, J.-H.; Kim, S.-O.; Hilton, D. L.; Cho, N.-J., Acid-catalyzed kinetics of indium tin oxide etching. *Thin Solid Films* **2014,** *565*, 179-185.

55. Schneider, C. A.; Rasband, W. S.; Eliceiri, K. W., NIH Image to ImageJ: 25 years of image analysis. *Nature Methods* **2012,** *9*, 671.

56. Shen, S.; Zhang, X.; Perdue, B.; Stickney, J., *Formation of CdS using electrochemical atomic layer deposition (E-ALD) and successive ionic layer adsorption reaction (SILAR)*. Electrochimica Acta, 2018, 271: 19-26

57. Zhang, X.; **Shen, S.;** Howell, P.; Cheng, W.; Mubeen, S.; Stickney, J.*. "Potential Pulse ALD for Room Temperature Fabrication of Stoichiometric CdTe Nanofilms" *Journal of The Electrochemical Society*, 2019, 166 (5): H3249-H3256

FIGURES

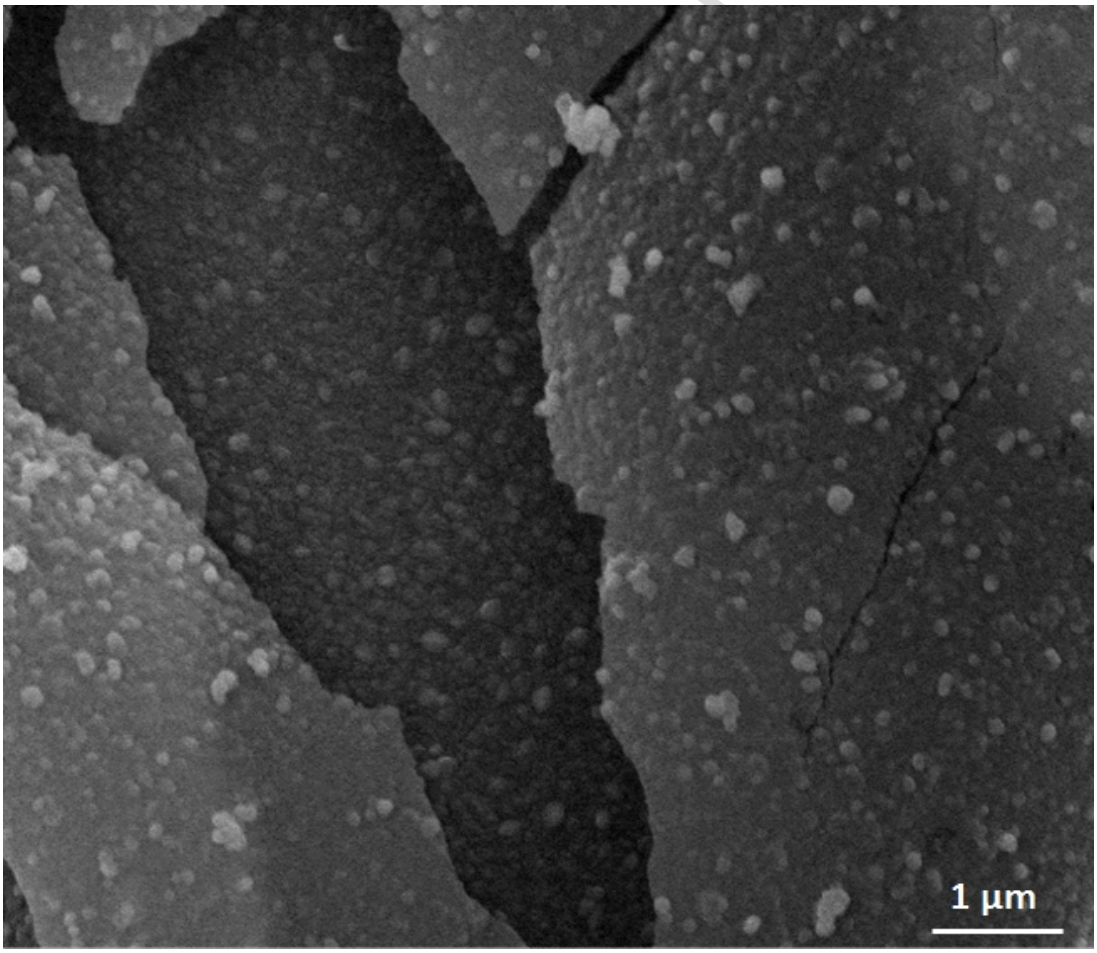

Figure 1. Scanning electron micrograph of CdS-CdTe delaminated from the ITO surface.

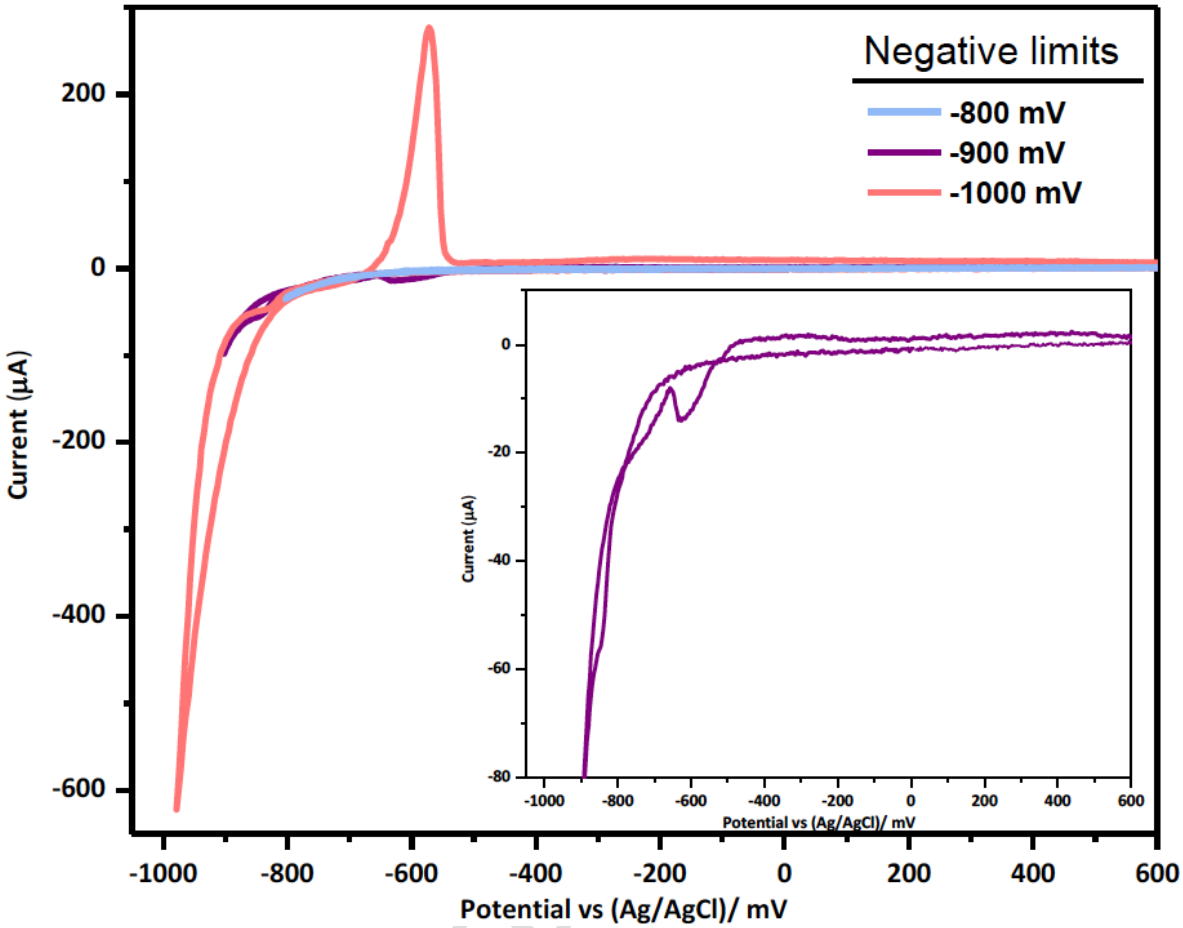

Figure 2. Current-vs-potential curves for ITO in 0.5 M $NaClO_4$ solution at pH 3, scanned initially in the negative direction from the open-circuit potential, 0.600 V. The scans were reversed towards the positive direction at -800 mV (blue), -900 mV (purple), and -1000 mV (red). The inset is an expanded view of the purple scan. The potential was measured against a Ag/AgCl (3 M KCl) reference electrode; the scan rate was 10 mV/s.

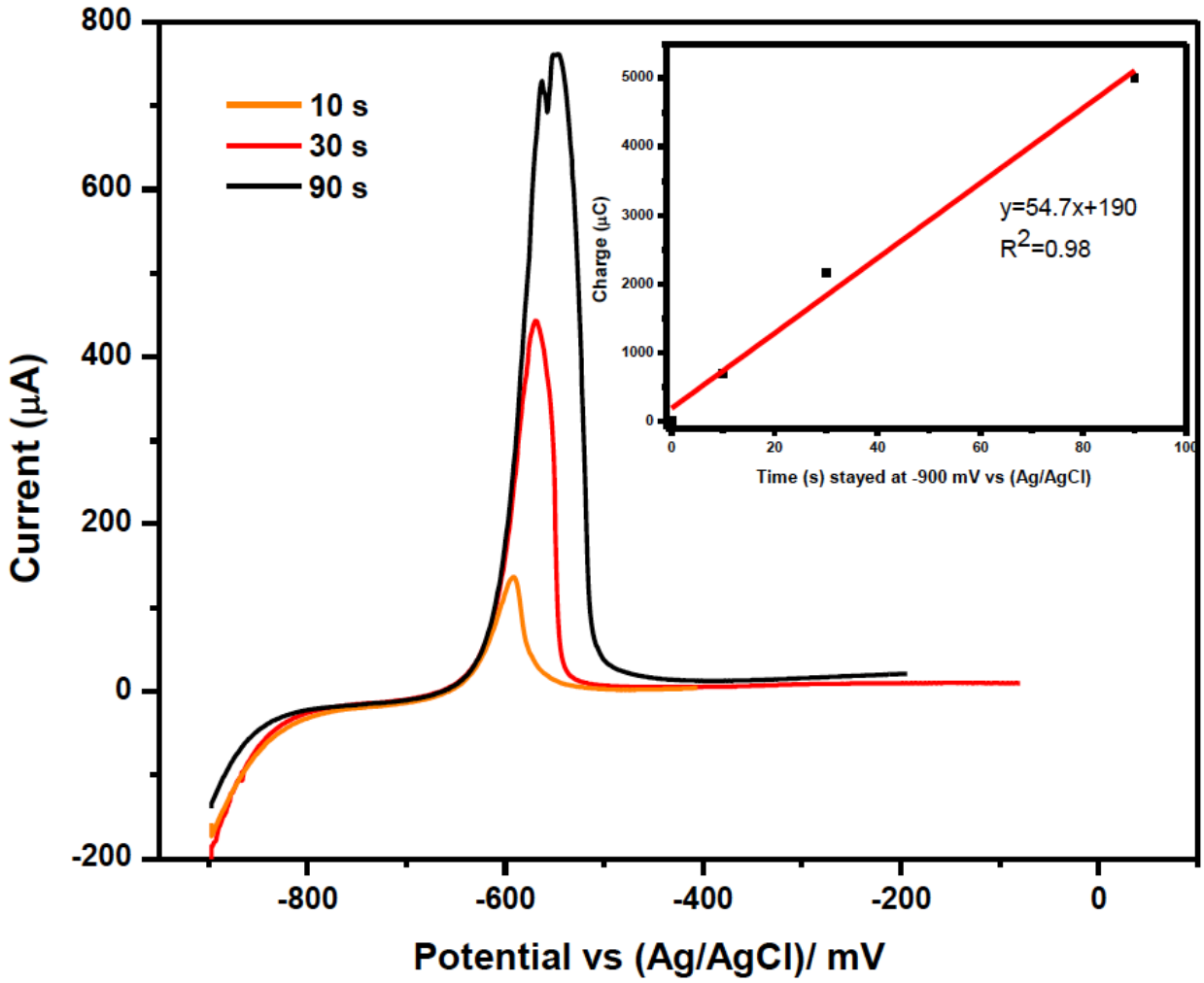

Figure 3. Linear sweep voltammetry scanned in the positive direction after ITO reduction at -900 mV for 10 s (orange), 30 s (red), and 90 s (black). The inset is the linear fit of the oxidation charge versus the reduction time. The potential was measured against the Ag/AgCl reference electrode; a scan rate of 10 mV/s was employed.

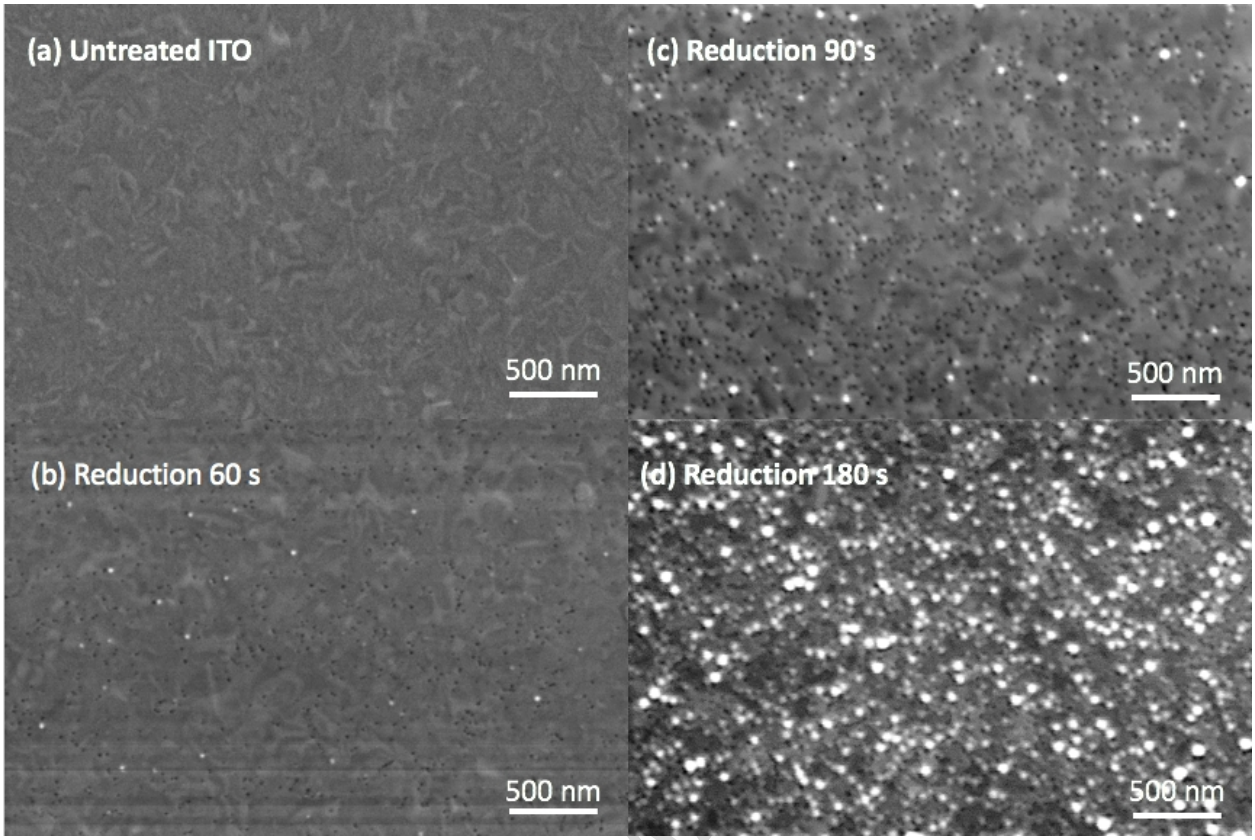

Figure 4. SEM of untreated ITO (a), compared with ITO reduced at -900 mV for (b) 60 s, (c) 90 s, and (d) 180 s. The acceleration voltage used was 10 keV.

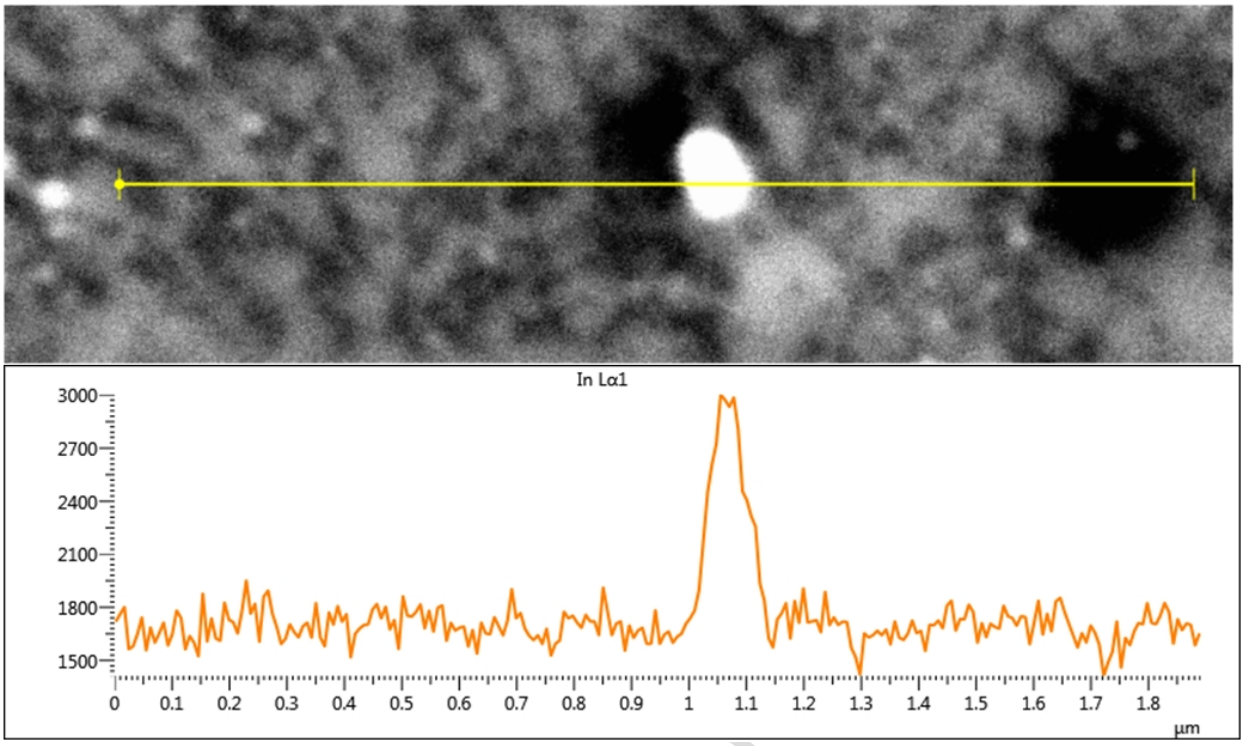

Figure 5. EDS line scan of a bright particle created by ITO reduction at -900 mV, showing high signals of In compared to those in the background.

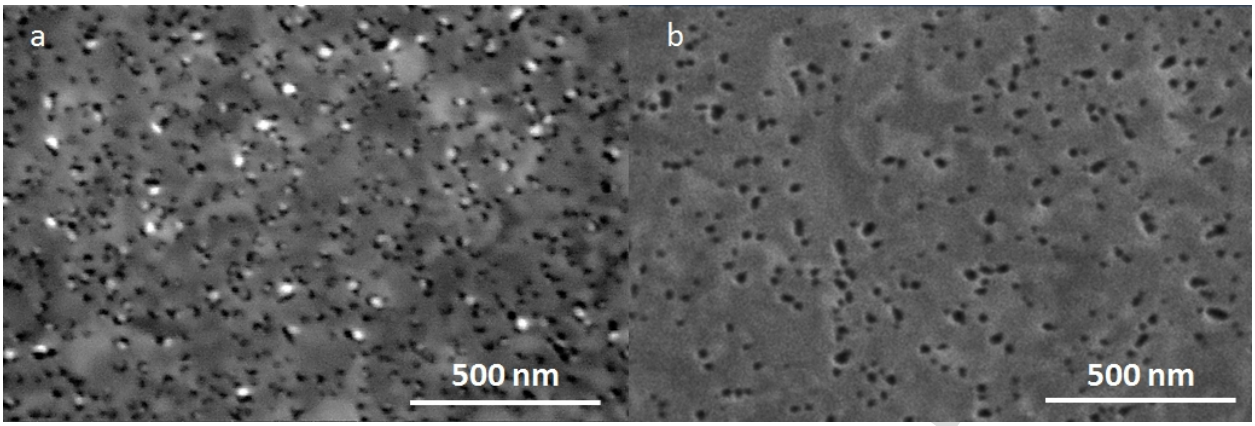

Figure 6. SEM of (a) ITO reduced at -900 mV for 90 s and immediately emersed from electrolytic solution; (b) ITO reduced at -900 mV for 90 s but left immersed in a non-electrolytic solution for 5 minutes.

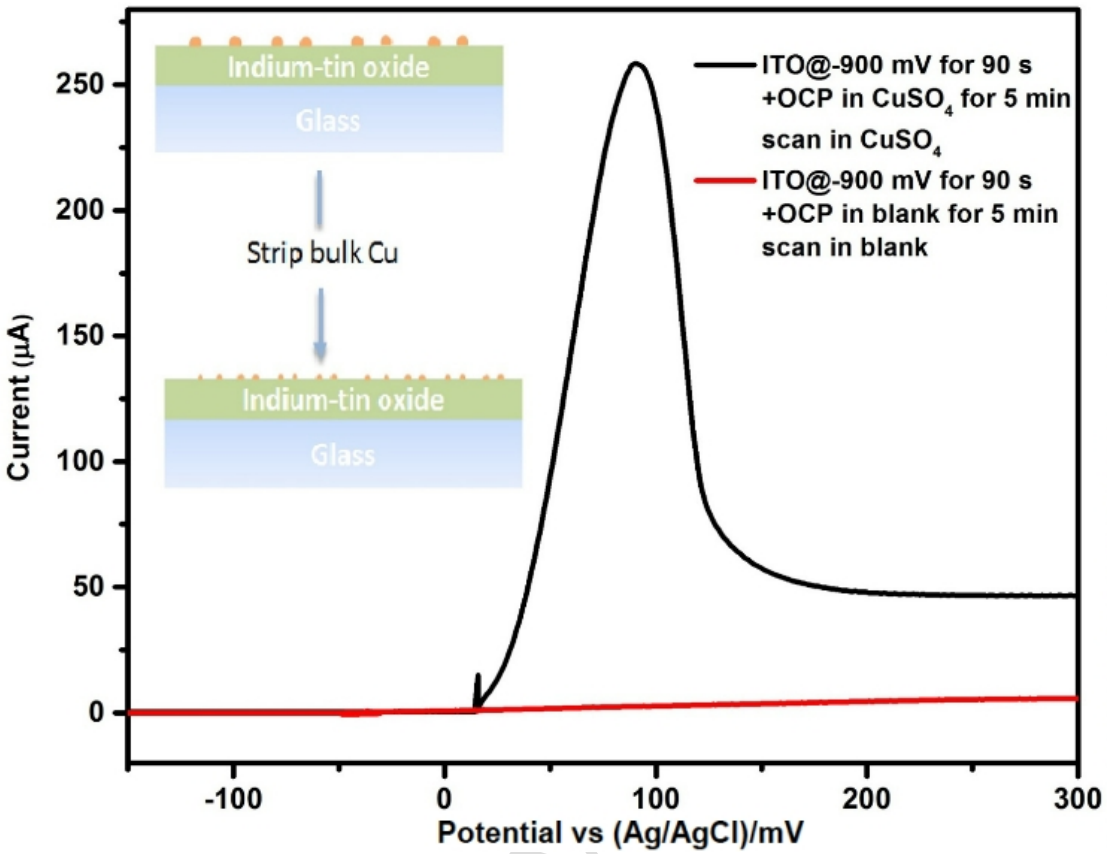

Figure 7. Black curve: anodic-direction voltammetric scan in $CuSO_4$ from the OCP after 5 minutes of Cu-by-In redox replacement on ITO pre-reduced for 90 seconds at -900 mV. Red curve: same as black scan except that pre-reduced ITO was left for 5 minutes at OCP in blank solution. The graphical illustration is that of bulk-Cu stripping at 200 mV to expose smaller nucleation sites.

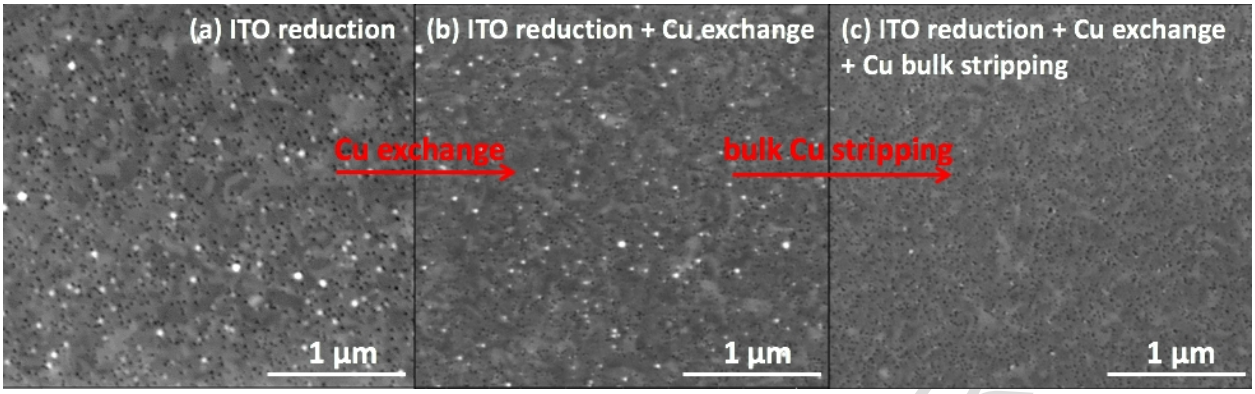

Figure 8. SEM of (a) ITO reduced at -900 mV for 90 s; (b) ITO reduced at -900 mV for 90 s followed by 5 min of Cu^{2+} redox displacement at OCP; (c) same treatment as (b) but scanning to 200 mV to strip bulk Cu.

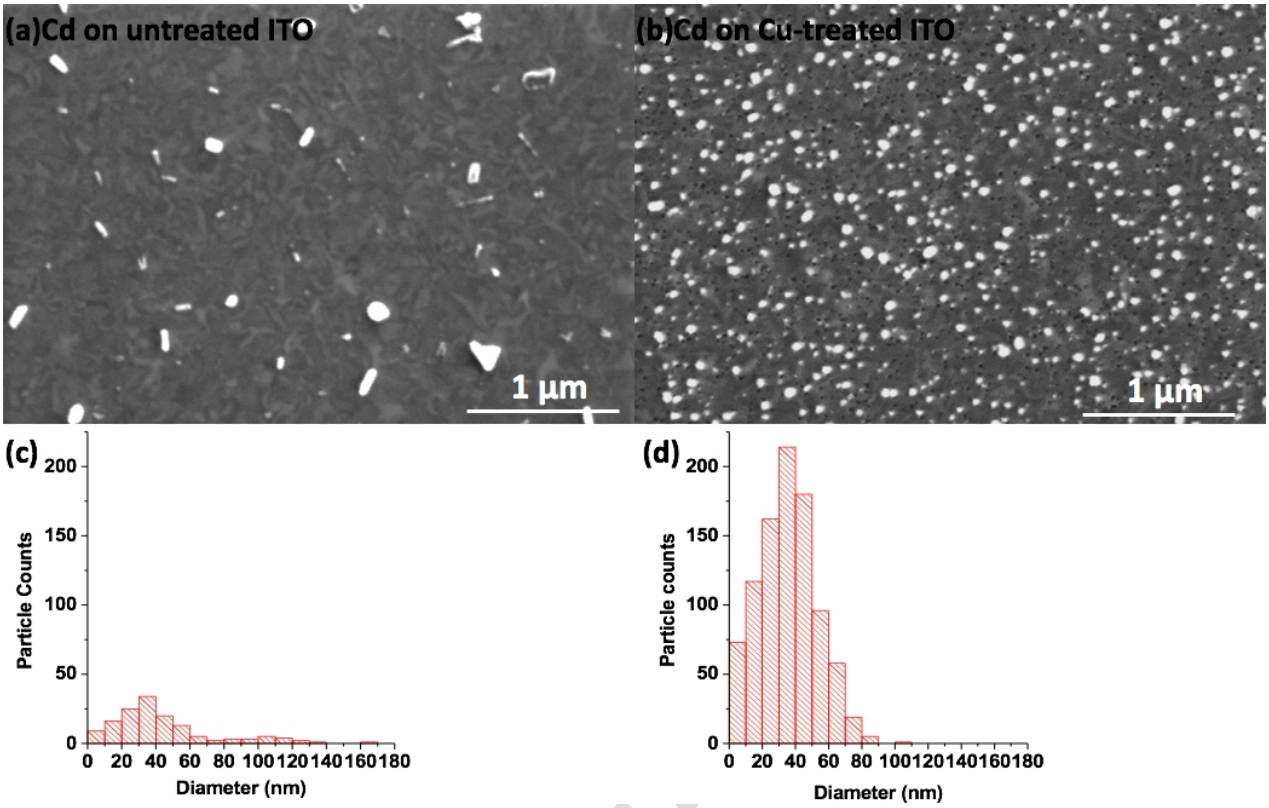

Figure 9. SEM of Cd deposition at -900 mV for 90 s on (a) untreated ITO and (b) Cu-treated ITO. Histograms (c) and (d) show the particle size distributions in (a) and (b), resepctively.

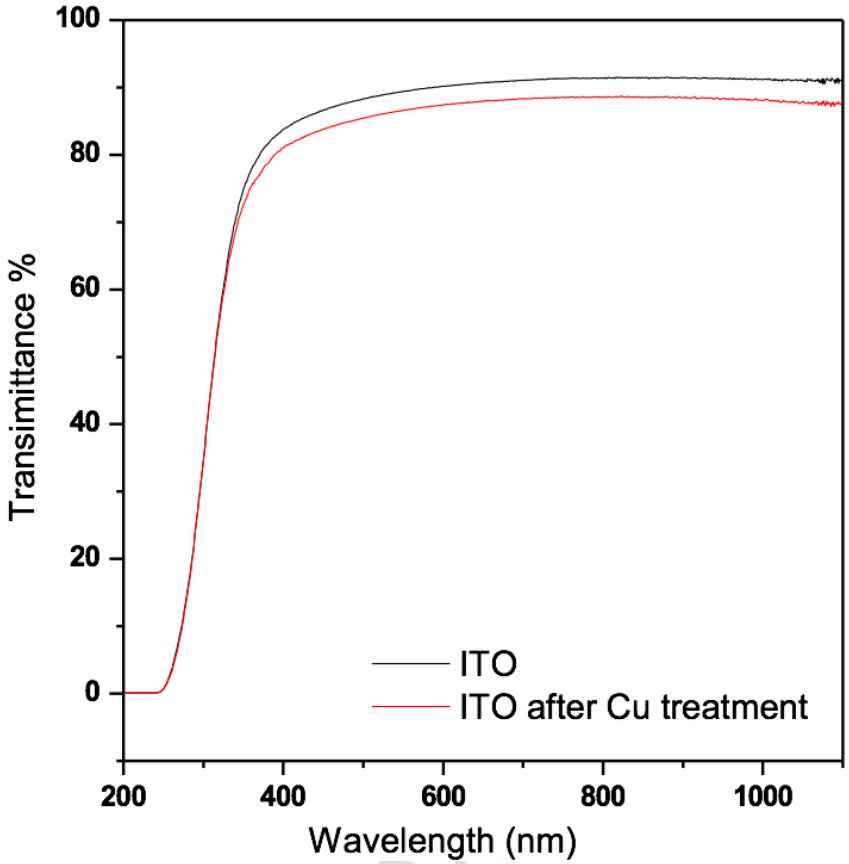

Figure 10. Transmittance spectrum of untreated ITO (black) and Cu-treated ITO (red).

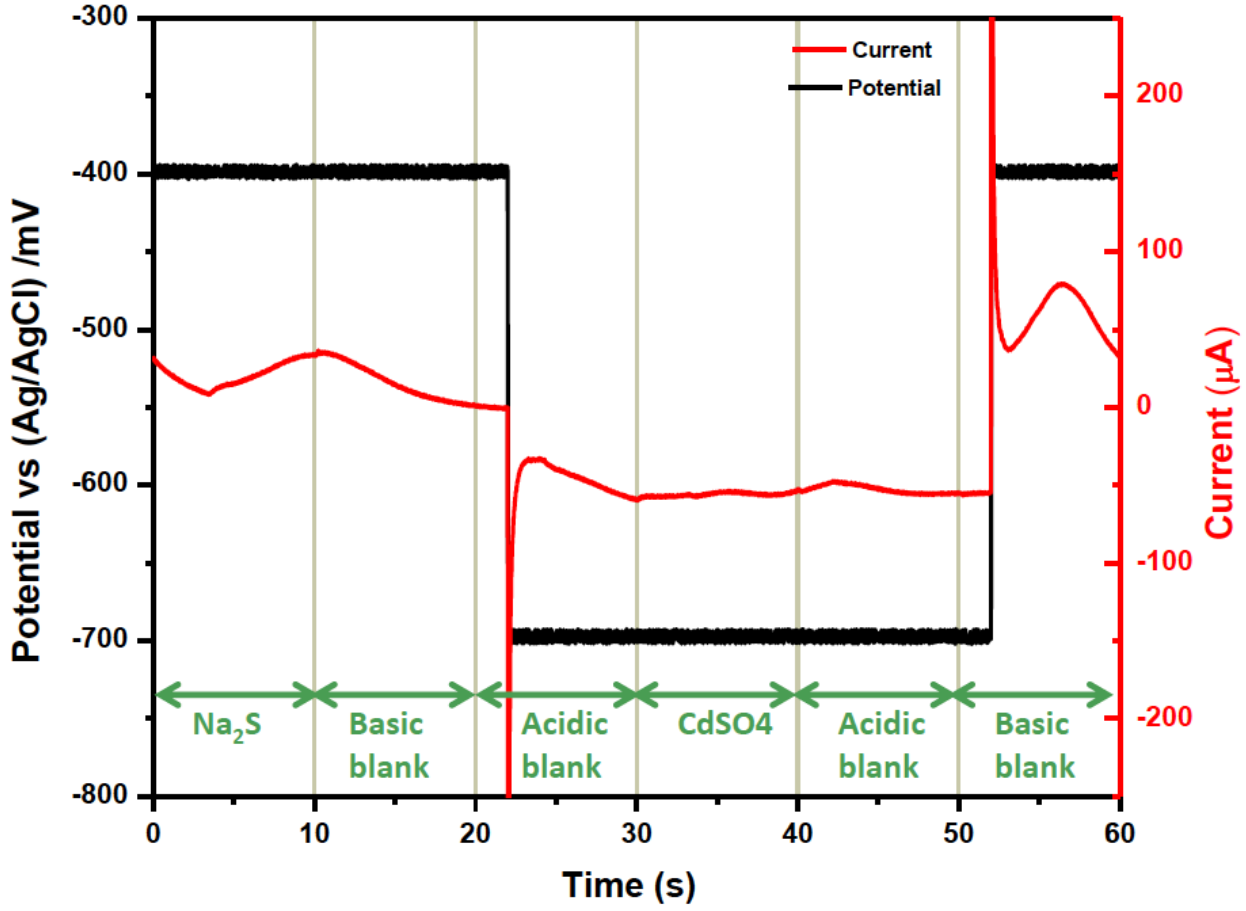

Figure 11. Potential-current-time trace of one complete CdS E-ALD cycle. The straight black lines represent the programmed potential, and the red curve is the corresponding current. The solution in the cell corresponding to each step is indicated in the green-highlighted ttext.

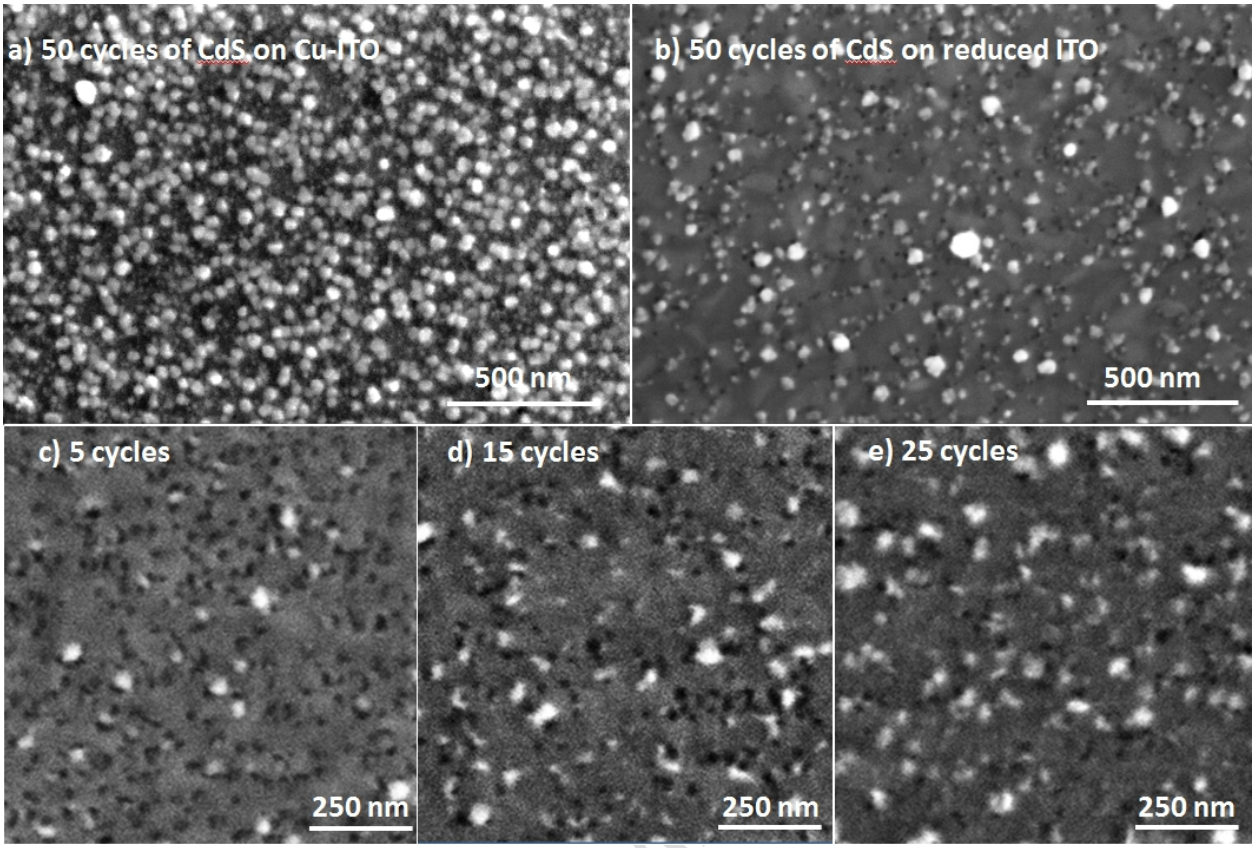

Figure 12. SEM of (a) 50 cycles of CdS deposition on a Cu-treated ITO, (b) 50 cycles of CdS deposition on ITO reduced at -900 for 90 s but without any Cu displacement. (c-e) 5, 15, 25 cycles of CdS deposition on a Cu-treated ITO, respectively

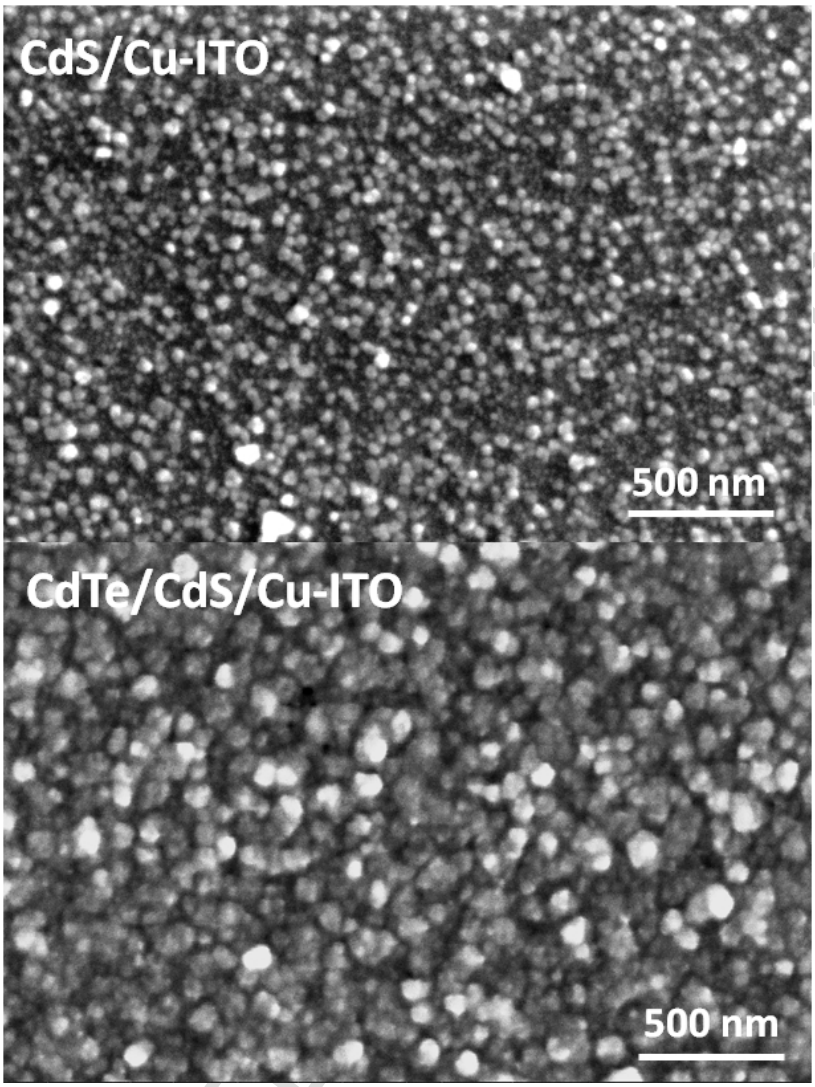

Figure 13. SEM of 50-cycles of CdS/Cu-ITO deposition before and after 90-cycles of pulse-plated CdTe (PP-ALD).